G. T. Hahn[1] *and A. R. Rosenfield*[1]

Sources of Fracture Toughness: The Relation Between K_{Ic} and the Ordinary Tensile Properties of Metals

REFERENCE: Hahn, G. T. and Rosenfield, A. R., "**Sources of Fracture Toughness: The Relation between K_{Ic} and the Ordinary Tensile Properties of Metals**," *Applications Related Phenomena in Titanium Alloys, ASTM STP 432*, American Society for Testing and Materials, 1968, pp. 5–32.

ABSTRACT: This paper examines crack extension from a metallurgical standpoint. Stress and strain intensification at the crack tip and the basic flow and fracture properties of the material are considered. Insights derived from etch-pitting experiments are reviewed. These reveal the two characteristic types of local yielding: (1) plane strain or "hinge-type" relaxation and (2) plane stress or through-the-thickness relaxation. Two simplified elastic-plastic treatments that model plane strain and plane stress are identified. They offer approximate equations connecting K (the stress intensity parameter) with the plastic zone size and the crack-tip displacement, which are in good accord with experiment. They also help to define limiting conditions for plane strain and plane stress. A method of relating the crack-tip displacement to the peak strain is described, and this is combined with a critical strain criterion for ductile fracture. In this way, the plane strain fracture toughness parameter K_{Ic} is formulated in terms of ordinary tensile properties: $K_{Ic} \approx \sqrt{\frac{2}{3}EYn^2\epsilon^*}$ (E is the modulus, Y the yield stress, n the strain hardening exponent, and ϵ^* the true strain at fracture of a smooth tensile bar). This expression is shown to be in good accord with available data on a variety of titanium, aluminum, and steel alloys. Since the influence of composition and heat treatment on tensile properties is already established in many cases, the tensile properties can now serve as a link between fracture toughness and the backlog of metallurgical experience. This possibility is demonstrated for Type 4340 steel heat treated to different strength levels.

KEY WORDS: crack extension, fracture toughness, plastic flow, tensile properties, testing, metals, ductility, crack-tip displacement, stress gradient, strain hardening

Irwin's concept of fracture toughness has been the subject of many papers and seminars. Ways of measuring K_{Ic} and K_c and the factors that correct for end effects and special shapes are finding their way into the literature [*1*].[2] However, virtually nothing has been said about the origins

[1] Metal Science Group, Battelle Memorial Institute, Columbus Laboratories, Columbus, Ohio.

[2] The italic numbers in brackets refer to the list of references appended to this paper.

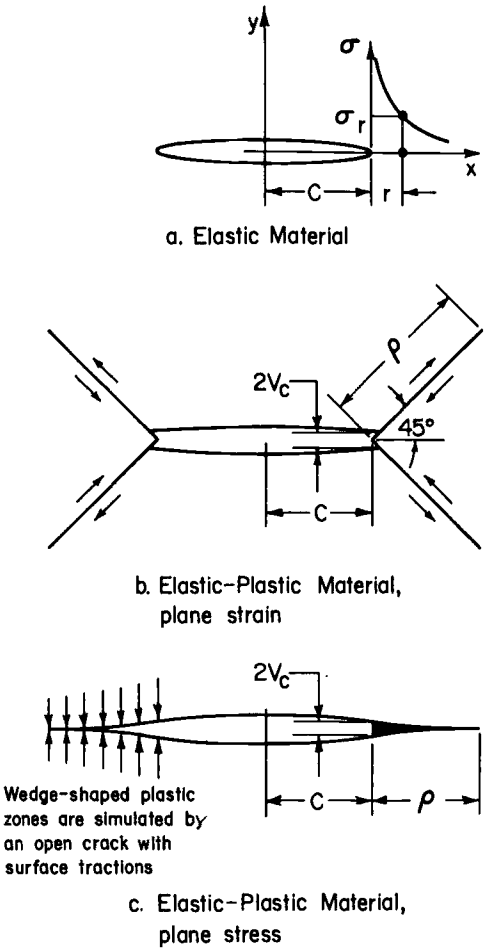

FIG. 1—*Models of a stressed crack:* (a) *Inglis* [3] *model for an elastic material,* (b) *Bilby-Swinden* [4,5] *model for plane strain relaxation in an elastic-plastic material, and* (c) *Dugdale-Muskhelishvili* [6] *model for plane stress relaxation in an elastic-plastic material.*

of crack extension resistance. What basic metallurgical factors contribute to the toughness of an alloy? How can composition, processing, and heat treatment be manipulated to enhance the value of K_{Ic} ? Answers to these questions would not only benefit alloy development but would simplify quality control and the task of preparing specifications.

The metallurgy of crack extension resides in the small region ahead of a crack that yields, flows, and ultimately ruptures. This region has been inaccessible in the past. It could not be measured, and it could not be dealt with analytically. Now, more and more studies are penetrating the plastic zone. Recent advances already contain insights useful to the metallurgist.

This paper consolidates findings about the yielded region that point to the metallurgical origins of fracture toughness. The paper draws on theory and experiments to construct simplified pictures of plane strain and plane stress plastic relaxation. Measurements and analytical results are combined, and these define quantitative relations between K_{Ic} and K_c and the ordinary tensile properties of metals: the elastic modulus, yield stress, strain hardening index, and the true strain at fracture. Since the influence of composition and heat treatment on tensile properties is already established in many cases, the tensile properties become a link between fracture toughness and the backlog of metallurgical experience. This paper confines itself to ductile fracture modes. A possible treatment of cleavage has been proposed elsewhere [*2*]. Cyclic loading

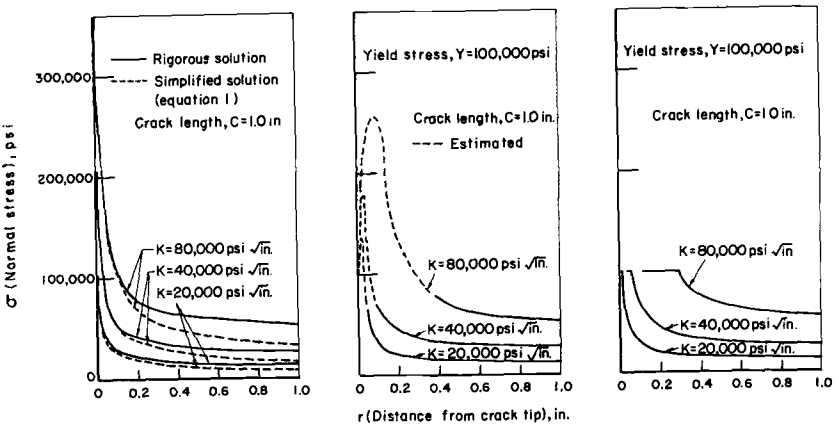

FIG. 2—*Stress gradients ahead of a sharp crack:* (a) *elastic material,* (b) *nonwork hardening elastic-plastic material under plane strain* [9] *and* (c) *nonwork hardening elastic-plastic material under plane stress* [11].

and environmental effects are also very important but are beyond the scope of the present treatment.

Significance of K, K_{Ic}, and K_c

Irwin's [*1*] concept of stress intensity and fracture toughness—the parameters K, K_{Ic}, and K_c—stem from the following expression for the stress ahead of a sharp crack in a linear elastic material (Fig. 1):[3]

$$\sigma = T\sqrt{\pi C}\,(2\pi r)^{-1/2} \quad \ldots\ldots\ldots\ldots\ldots\ldots (1)$$

[3] The term σ is the normal stress a distance r in front of the crack (see Fig. 1*a*), T is the nominal applied stress, and $2C$ is the crack length. Equation 1, a simplified version of the Inglis solution for a crack in an infinite plate, is only valid close to the crack tip (when $r \lesssim 0.5\,C$) provided there is no plastic relaxation. The rigorous form of the Inglis [*3*] solution for a sharp crack is: $\sigma/T = \mathrm{Coth}\,\alpha$, $\mathrm{Cosh}\,\alpha = x/C$, and this is compared with the simplified version in Fig. 2*a*.

TABLE 1—*Approximate relations valid near the crack tip.*

Elastic Material[a]	Elastic-Plastic Material[b]
$r_{(\sigma)} \propto K^2$	$\rho \propto (K/Y)^2$
$\sigma_{(r)} \propto K$	$\sigma_{r>\rho} \propto K$
	$\sigma_c = Y$
	$\sigma_{max} = f[Y, (K/Y)^2\ 1/t]$
$\epsilon_{(r)} \propto K/E$	$\epsilon_{max} = f[K/Y, (K/Y)^2\ 1/t, E, n]$
	$v_c \propto (Y/E)(K/Y)^2$
$We \propto K^2C/E$	$W_p \propto (Y^2/E)\ (K/Y)^4$
$dWe/dC \sim G \propto K^2/E$	

[a] Derived from Eq 1.

[b] Based on the Bilby-Swinden [*4*] and Dugdale-Mushkelishvili [*6*, *11*] treatments, and valid at low stress levels (that is, when $T/Y < 0.7$)

$K \equiv T\sqrt{\pi C}$,
T = nominal applied stress,
$2C$ = crack length,
Y = yield stress,
E = Young's modulus,
$r_{(\sigma)}$ = distance corresponding to σ,
ρ = plastic zone size,
n = strain hardening index,
t = plate thickness,
$r = (x - c)$,
$\sigma_{(r)}$, $\epsilon_{(r)}$ = stress and strain front of the crack at, $x = r + c$, $y = 0$,
σ_c = crack-tip normal stress,
σ_{max} = the peak normal stress,
ϵ_{max} = the peak crack tip tensile strain,
v_c = crack tip displacement,
W_e = stored elastic energy,
W_p = stored plastic energy, and
G = elastic energy release rate.

The term $T\sqrt{\pi C}$ has special properties—it is proportional to σ and reflects an equivalence between the effects of T and $\sqrt{C}$—and is given special names:

$$K \equiv \text{stress intensity parameter}^4 \equiv T\sqrt{\pi C} \quad (2)$$

[4] The matter of terminology is confused because McClintock and Irwin [*7*] define K_{Ic} as the Mode I fracture toughness parameter but do not make it clear how to distinguish between (1) plane strain, (2) plane stress, (3) the onset of slow growth, and (4) the onset of unstable propagation. We use the following definitions in this paper for Mode I because they are close to general practice and still make the necessary distinctions:

K_{Ic} = stress intensity (value of K) at the onset of slow (stable) crack growth under *plane strain*. T^* is the corresponding value of applied gross section stress.

K_c = stress intensity at the onset of slow (stable) crack growth when the state of stress throughout the loading has been predominantly *plane stress*.

The reader should also note that the relation K_{Ic}, $K_c \equiv T^* \sqrt{\pi C}$ is valid for a small centrally located through-crack in a large plate, that is, $2C$ is smaller than $\frac{1}{10}$ the width dimension. For larger cracks, edge cracks or different geometries the proper relation is K_{Ic}, $K_c = \varphi T^* \sqrt{\pi C}$ where φ is a correction factor for the particular configuration [*8*].

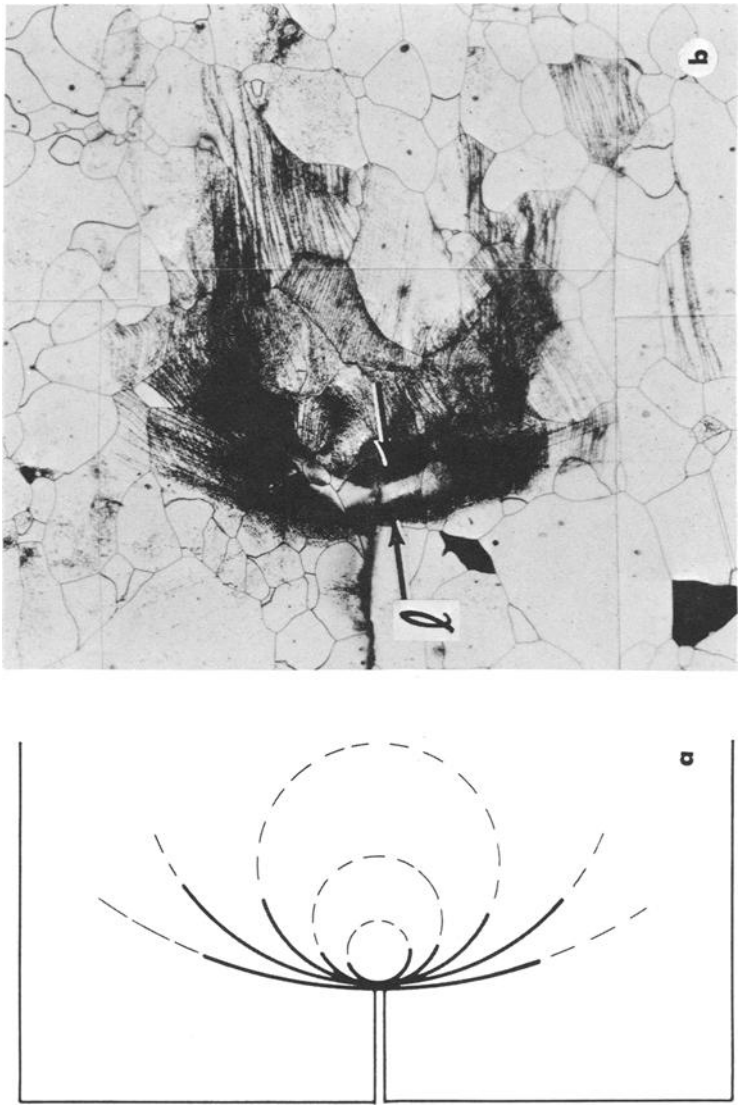

FIG. 3—*Plane strain relaxation:* (a) *schematic and* (b) *an actual zone revealed by etching an 0.060-in.-thick, precracked silicon steel plate after loading to* $K/Y = 0.25\sqrt{in.} = 1.27\sqrt{mm}$, $(K/Y)^2 1/t = 0.95$, $t_{(s)} \approx 0.002$ *in.* $= 0.5$ *mm* ($\times 200$).

$$K_{Ic} \equiv \text{plane strain fracture toughness} \equiv T^*\sqrt{\pi C} \quad \text{parameter (see footnote[4])} \quad \ldots\ldots(3)$$

$$K_c \equiv \text{plane stress fracture toughness} \equiv T^*\sqrt{\pi C} \quad \text{parameter (see footnote[4])} \quad \ldots\ldots(4)$$

The fracture toughness concept for an elastic material then follows from one additional step. A criterion for fracture is introduced: rupture occurs at the crack tip when a critical normal stress, $\sigma = \sigma^*$ is attained at a fixed distance r^*. The terms σ^* and r^* are regarded as basic properties of the material. This is combined with Eq 1, 3, or 4 and leads to the important conclusion:

$$T^*\sqrt{\pi C} \equiv K_{Ic}\,,\ K_c = \sigma^*\,(2\pi r^*)^{1/2} = \text{constant} \quad \ldots\ldots(5)$$

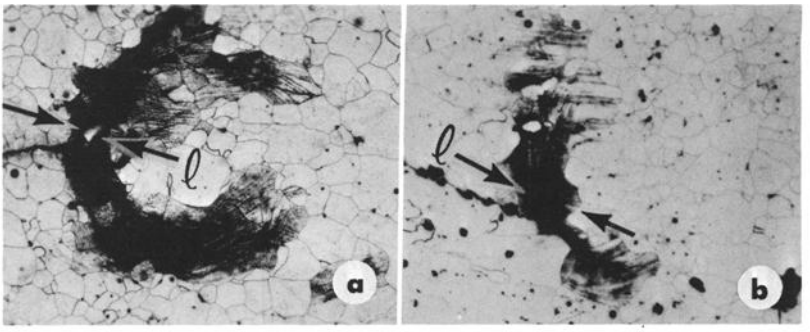

(a) Plate surface and (b) plate midsection, $K/Y = 0.3\ \sqrt{\text{in.}} = 1.51\ \sqrt{\text{mm}}$, $(K/Y)^2 1/t = 0.36$, $l_{(n)} \approx 0.002$ in. = 0.5 mm.

FIG. 4—*Examples of plane strain relaxation in precracked 0.250-in.-thick Fe-3Si steel plates revealed by etching after loading.*

In other words, K_{Ic} and K_c have several unique properties:

1. They are material constants independent of crack length.
2. They identify the conditions for crack extension—the critical stress level-crack length combinations.
3. They can be related to basic material parameters, for example, σ^* and r^*.
4. In principle, the value of K_{Ic} and K_c can be determined from a single experiment, which involves breaking a precracked specimen in the laboratory and measuring the applied stress at fracture.

Commercial alloys also display constant K_{Ic} and K_c values in spite of the fact that these alloys yield and relax plastically at the crack tip. It is surprising: (*a*) because Eq 1 does not describe the stresses in an elastic-plastic material (compare Fig. 2*a* with *b* and *c*), and (*b*) because the maximum stress criterion is inappropriate for the common ductile

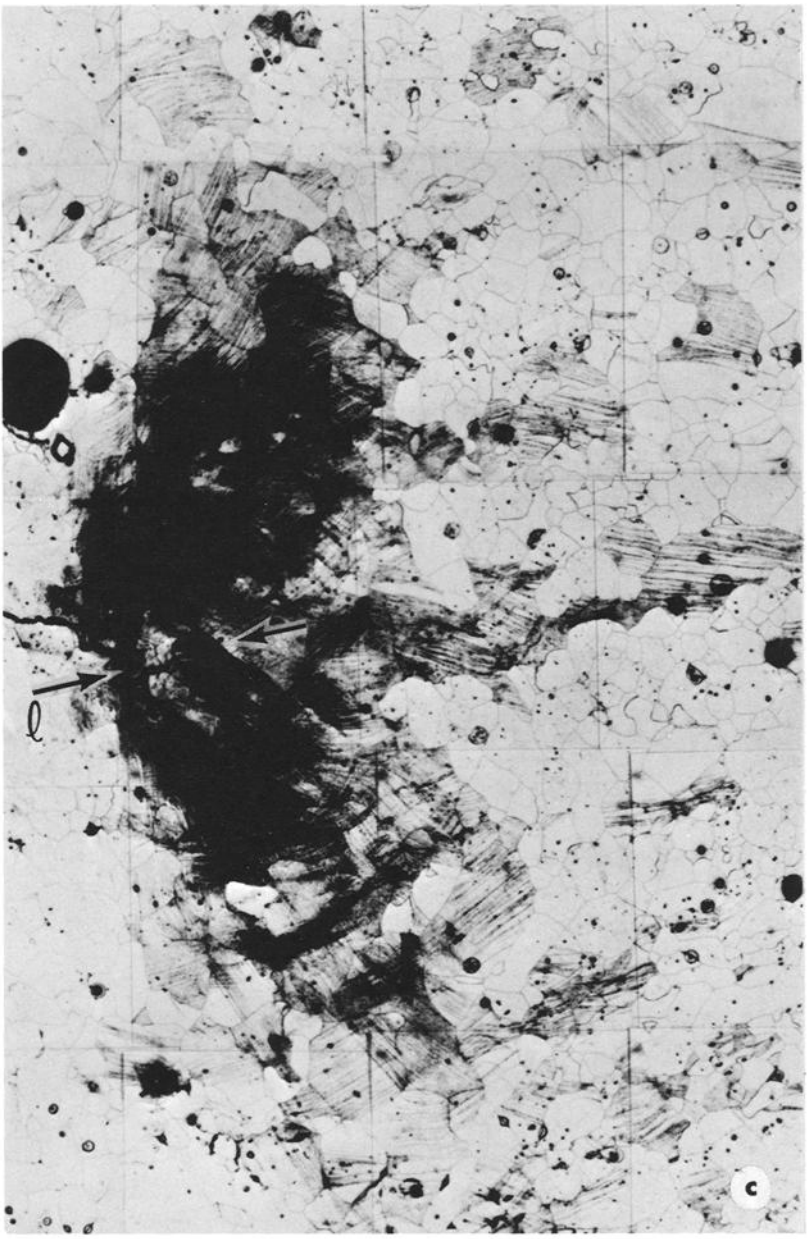

(c) Plate midsection, $K/Y = 0.45\ \sqrt{\text{in.}} = 2.3\ \sqrt{\text{mm}}$, $(K/Y)^2 1/t = 0.8$, $l_{(n)} \approx 0.005$ in. = 1.27 mm. (×100).

FIG. 4 (*c*)

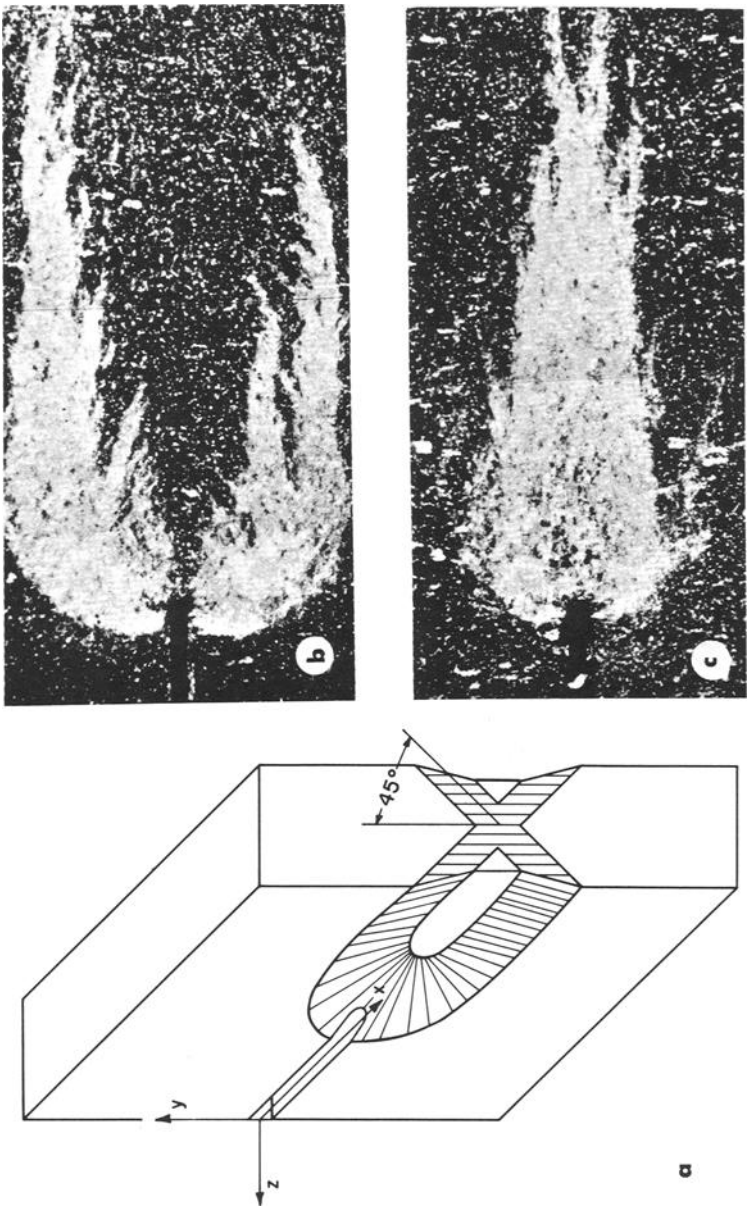

FIG. 5—*Plane stress relaxation:* (a) *schematic,* (b) *plate surface, and* (c) *plate midsection are an actual zone revealed by etching a 0.128-in.-thick edge-notched silicon steel plate after loading to* $K/Y = 0.76\sqrt{in.} = 3.9\sqrt{mm}$, $(K/Y)^2 t = 4.5$. *Oblique lighting* (×13.5).

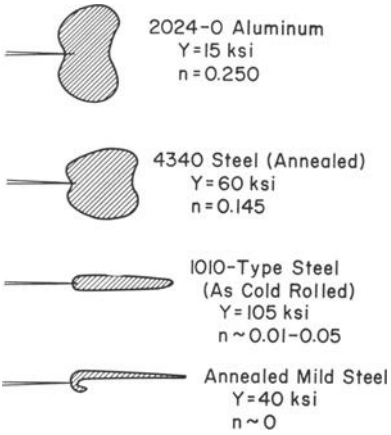

FIG. 6—*Plane stress plastic zone shapes observed by Gerberich* [12] *and the present authors. The zones are not drawn to the same scale.*

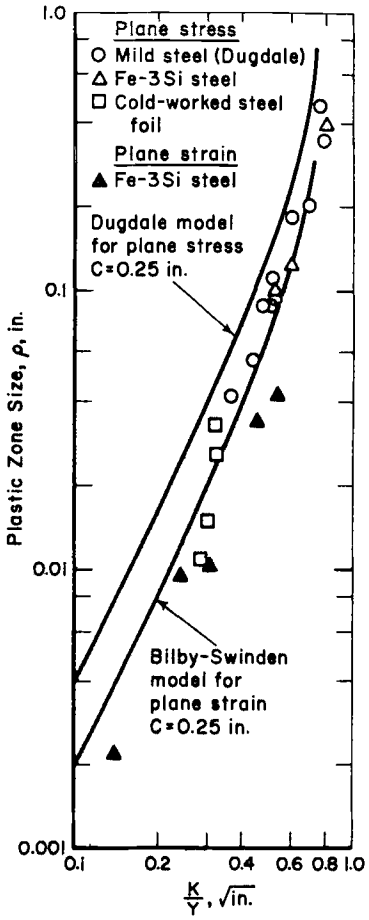

FIG. 7—*Comparison of plastic zone size values derived from the simple models* [4-6,11] *with experiments. Details are given in Table 2.*

modes of fracture [*10*]. At one time this ambivalence puzzled many workers, but it can now be understood in the light of several "pseudo" elastic-plastic crack tip analyses [*4–6,11*]. Two useful models are illustrated in Figs. 1*b* and *c*. These analyses are approximate because they

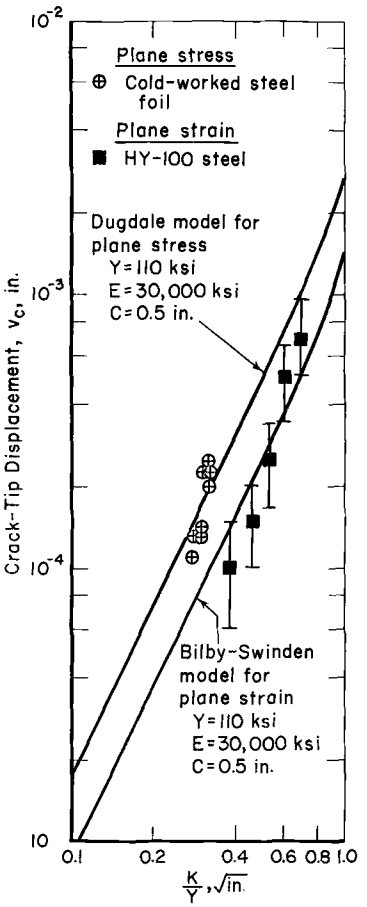

FIG. 8—*Comparison of crack tip displacement values derived from the sample models* [4–6,11] *with experiments. Details are given in Table 2.*

treat idealized plastic zones and neglect strain hardening, but they have the virtue of offering the relatively simple expressions listed in Table 1.

Table 1 illustrates that the general features of Irwin's elastic mechanics are also displayed by elastic-plastic solutions:

1. The term K continues to express the equivalence between applied stress and crack length (though only at low stress levels, that is, when $(T/Y) < 0.7$).

2. Such features as ρ, the plastic zone size, v_c the crack tip displacement, and ϵ_c the crack tip strain are monotonic—though not linear—

functions of K. This means that a fracture criterion based on a constant limiting value of either v_c or ϵ_c must lead to a constant value of K_{Ic} or K_c.

The simple elastic-plastic treatments also recognize an additional materials parameter: Y, the yield stress, but do not describe σ_{max} or ϵ_{max}, the peak tensile stress and strain at the crack tip, explicitly. These quantities depend on the exact geometry and on the strain hardening index, factors that are dealt with in the next two sections.

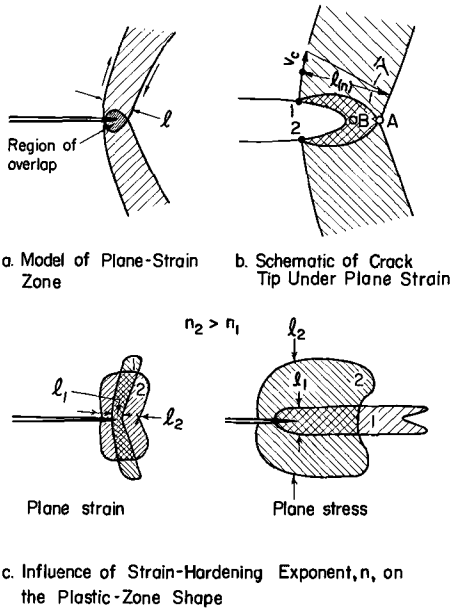

FIG. 9—*Schematic drawings of plane strain and plane stress plastic zones showing the influence of strain hardening.*

Plane Strain and Plane Stress Relaxation

Plastic relaxation at the crack tip takes two characteristic forms [*11*]:

Plane Strain—Figure 3 illustrates that the plastic zone has some of the features of a hinge when the zone is small relative to the plate thickness. Essentially no strains are observed in the thickness direction. The zone also has the same appearance on interior sections parallel to the plate surface (see Fig. 4). This implies that the plastic displacements are the same on the surface and on interior sections and that the displacement vectors are parallel to the plate surface, or, in other words, that the plastic relaxation is plane strain.

The two regions of shear on either side of the crack resemble the simple model (Fig. 1*b*). In both cases the extent of the zone—the distance ρ—becomes larger as K is increased. Note that the idealized zone (Fig. 1*b*) confines the shear to a single slip plane inclined at 45 deg,

TABLE 2—*Description of zone size and displacement measurements.*

Material	Y,[c] ksi	n	t, in.[c]	Zone Type	$(K/Y)^2\ 1/t$	Quantity Measured	Technique	Reference
Fe-3Si steel	68	0.0 to 0.2[b]	0.060 to 0.400	plane strain	0.01 to 0.9	ρ	etching internal surface	[a]
HY-100 steel	109	~0.1	0.348	plane strain	0.5 to 1.4	ν_c	moiré pattern on surface	[a]
Fe-3Si steel	64	0.0 to 0.2[b]	0.017	plane stress	15 to 37	ρ	etching	[12]
Mild steel (annealed)	26	~0.0	0.050	plane stress	2.6 to 13	ρ	Lüders bands observed on surface	[6]
Mild steel (cold worked)	105	0.01 to 0.05	0.002	plane stress	~50	ρ, ν_c	interferometry	[a]

[a] Unpublished work by the authors.
[b] The stress-strain curve for this material displays a Lüders extension ($n \approx 0$) followed by work hardening ($n \approx 0.2$).
[c] These data may be expressed in metric form by multiplying stress in ksi by 0.7031 to obtain kgf/mm^2 and inches by 25.4 to obtain mm.

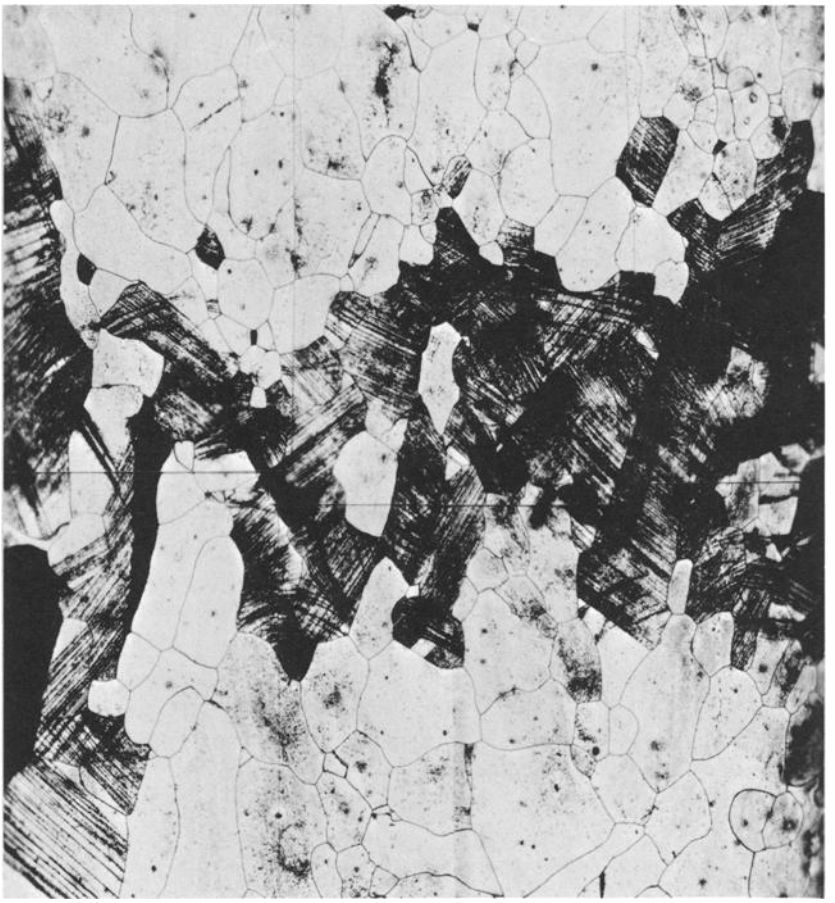

FIG. 10—*The central portion of the etched cross section of the plastic zone reproduced in Fig. 3*b. *Etching reveals some through-the-thickness deformation even though the relaxation is predominantly plane strain, for example*, $(K/Y)^2 1/t = 0.95$ ($\times 200$).

while the real zones poses a finite width and an inclination closer to 75 deg. Real zones are, in fact, quite narrow close to the crack tip. This is important because the zones accommodate relatively large displacements, and this means that they also harbor intense plastic strains.

Another feature of the plane strain zone is the constraint imposed on it by the surrounding elastic matrix. This produces a triaxial stress state in the interior of the plate which can support normal stresses as high as 2.7 Y.[5]

[5] Plasticity theory suggests that maximum constraint $\sigma_{max}/Y = 2.7$ is attained ahead of a sharp crack as soon as the plastic zone appears. On the other hand, a special interpretation of experimental data has suggested to the authors that the constraint develops gradually [9]: $(\sigma_{max}/Y) \approx 1 + 2(K/Y)$. This relation, consistent with crack length expressed in inches, was used to construct Fig. 2*b*, but it is open to question.

Plane Stress—When the extent of the hinge zone is comparable to the plate thickness, shear on planes inclined at 45 deg can penetrate the plate. Through-the-thickness deformation then supplants the hinges, and this is illustrated in Fig. 5. This form of relaxation cannot support stresses normal to the plate surface. For this reason, the triaxial stress state decays to a biaxial or plane stress state. In contrast to the plane strain zone, peak stress values here cannot be greater than the yield or flow stress, and this is shown in Fig. 2*b*.

Another important difference is that the width of the plane stress zone is relatively free to spread out normal to the tensile axis. The same crack-tip displacement, therefore, will produce a smaller strain concentration under plane stress than under plane strain. However, the zone can be quite narrow even under plane stress when the material does not strain harden, for example, when it diplays a Lüders' extension. Such narrow wedge-shaped zones are illustrated in Fig. 6*d* and closely resemble the Dugdale model.

Plane strain and plane stress represent two extremes that describe some, but bracket most, of the situations encountered in practice. They are useful concepts because they are associated with the lower and the upper limit of toughness and because they are easier to deal with analytically. Figures 7 and 8 compare, with experiments, the following theoretical expressions for ρ and v_c, the zone size and crack-tip displacement derived from the simple elastic-plastic models [*4,5,11*] (Fig. 9):[6]

[6] The curves drawn in Figs. 7 and 8 are actually derived from the more complete forms of these expressions:

$$\rho_{(\text{plane strain})} = \frac{C}{2}\left[\sec\left(\frac{\pi T}{2Y}\right) - 1\right] \quad \ldots\ldots (6a)$$

$$\rho_{(\text{plane stress})} = C\left[\sec\left(\frac{\pi T}{2Y}\right) - 1\right] \quad \ldots\ldots (7a)$$

$$v_{c(\text{plane strain})} = \frac{2YC}{\pi E} \ln \sec\left(\frac{\pi T}{2Y}\right) \quad \ldots\ldots (8a)$$

$$v_{c(\text{plane stress})} = \frac{4YC}{\pi E} \ln \sec\left(\frac{\pi T}{2Y}\right) \quad \ldots\ldots (9a)$$

which reduce to Eqs 6 to 9 at low stress levels, that is, when $T/Y < 0.7$. At the high stress levels, the equivalence between T and $\sqrt{C}$ expressed by K is not obeyed. Also note that while the quantities ρ and v_c are clearly defined for the simple models, their meaning becomes fuzzy when the zone is spread out. The experimental values quoted here are defined in Figs. 1 and 9. The value of v_c under plane strain is the plastic part of the displacement at the edge of the zone (between the Points 1 and 2 in Fig. 9*b*). Under plane stress it is the plastic part of the displacement across the entire enclave at the crack tip (marked I_1 and I_2 in Fig. 9*d*). Since the materials described here work harden little (HY-100 steel is the exception), the zones are narrow and the two sets of definitions are nearly the same.

$$\rho_{(\text{plane strain})} \approx \frac{\pi}{16}\left(\frac{K}{Y}\right)^2 \quad \ldots\ldots\ldots\ldots\ldots\ldots (6)$$

$$\rho_{(\text{plane stress})} \approx \frac{\pi}{8}\left(\frac{K}{Y}\right)^2 \quad \ldots\ldots\ldots\ldots\ldots\ldots (7)$$

$$v_{c(\text{plane strain})} \approx \frac{Y}{4E}\left(\frac{K}{Y}\right)^2 \quad \ldots\ldots\ldots\ldots\ldots\ldots (8)$$

$$v_{c(\text{plane stress})} \approx \frac{Y}{2E}\left(\frac{K}{Y}\right)^2 \quad \ldots\ldots\ldots\ldots\ldots\ldots (9)$$

Relatively few systematic measurements of these quantities have been reported so far, especially values reflecting predominantly plane strain

TABLE 3—*Estimates of limiting conditions for plane strain and plane stress relaxation and fracture.*

Type	ρ	$(K/Y)^2\,1/t$
Plane Strain:[a]		
Relaxation and fracture	$<t/4$, $<t/10$[d]	<1.3, <0.4[d]
Plane Stress:		
Relaxation[b]	$>2t$[e]	>5.2
Fracture[c]	$>4t$[e]	>10.4

[a] Deformation is and fracture is preceded by predominantly plane strain relaxation, and there is no significant loss of constraint as a result of through-the-thickness relaxation.

[b] Transition to plane stress state is substantially complete, although distribution of strain within plastic zone is still influenced by prior plane strain relaxation.

[c] Deformation and stress history preceding fracture is predominantly plane stress.

[d] More conservative limits proposed by Brown and Srawley [*16*] to assure a plane strain fracture with no loss of constraint.

[e] Plane stress zone size.

or plane stress relaxation that are not complicated by slow crack growth. The measurements quoted here are described more fully in Table 2. They show that Eqs 6 to 9 are not only sound qualitative guidelines but can also offer reasonably good quantitative descriptions. Additional evidence along these lines has been reported by Wells [*13*], who first drew attention to the connection between v_c and K, and also by Tetelman [*14*]. These conclusions are based on materials that display little or no strain hardening. The equations may have to be modified for materials that strain harden extensively.

Etching reveals that the transition from plane strain to plane stress is a gradual process. For example, Fig. 10, a section normal to the zone reproduced in Fig. 3*b*, shows evidence of through-the-thickness deformation at a stage where $\rho_{(\text{plane strain})} = t/6$ (t is the plate thickness). Even Fig. 4 shows evidence of some through-the-thickness deformation, and here $\rho_{(\text{plane strain})} = t/25$. Through-the-thickness deformation does

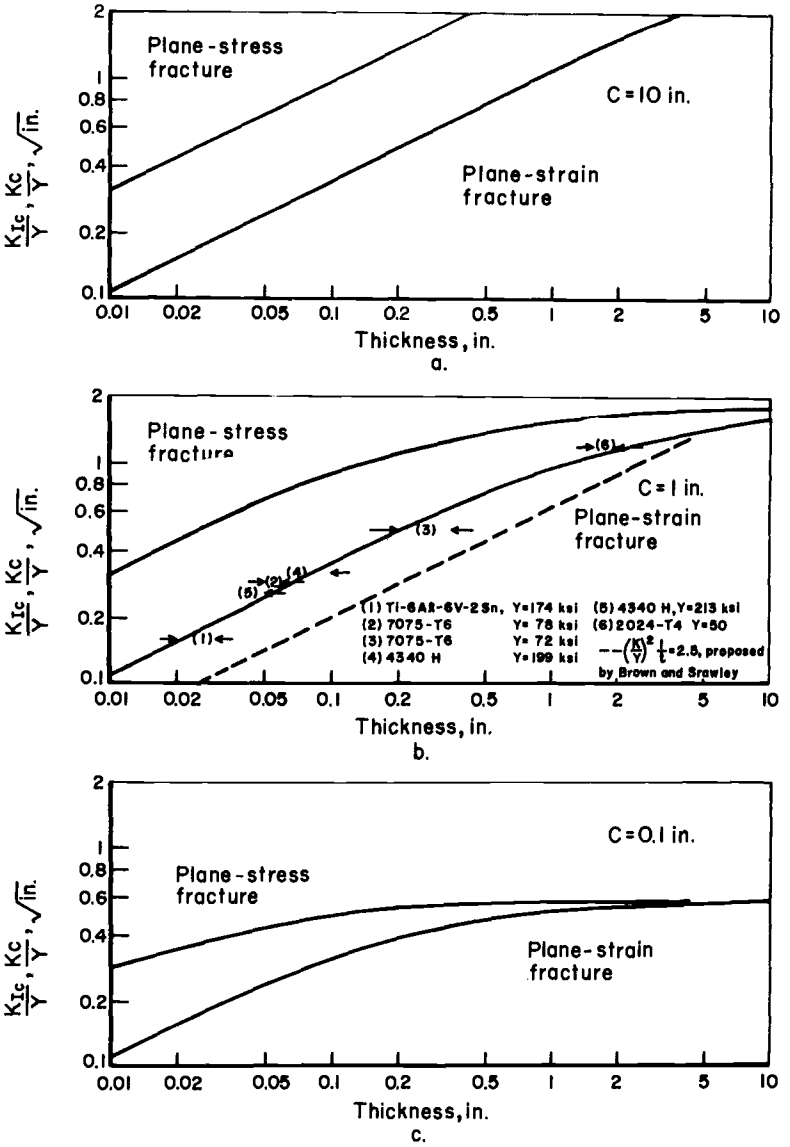

FIG. 11—*Limits for plane strain and plane stress fracture calculated for* (a) $C = 10$ *in. 25.4 mm,* (b) $C = 1.0$ *in. 2.54 mm, and* (*c*) $C = 0.1$ *in. 0.254 mm. Arrows identify the thickness range within which fracture toughness values measured by Irwin* [15] *and Brown and co-workers* [17] *begin to increase with decrease in plate thickness.*

become noticeable when $\rho_{(\text{plane strain})} = t/2$, and this means that it begins to detract sooner from plane strain relaxation and the attending triaxiality. On this basis $\rho_{(\text{plane strain})} = t/4$ is a reasonable first estimate of the beginning of a significant shift away from plane strain. This condition, equivalent to $(K/Y)^2\ 1/t = 1.3$ at low stress levels, is shown

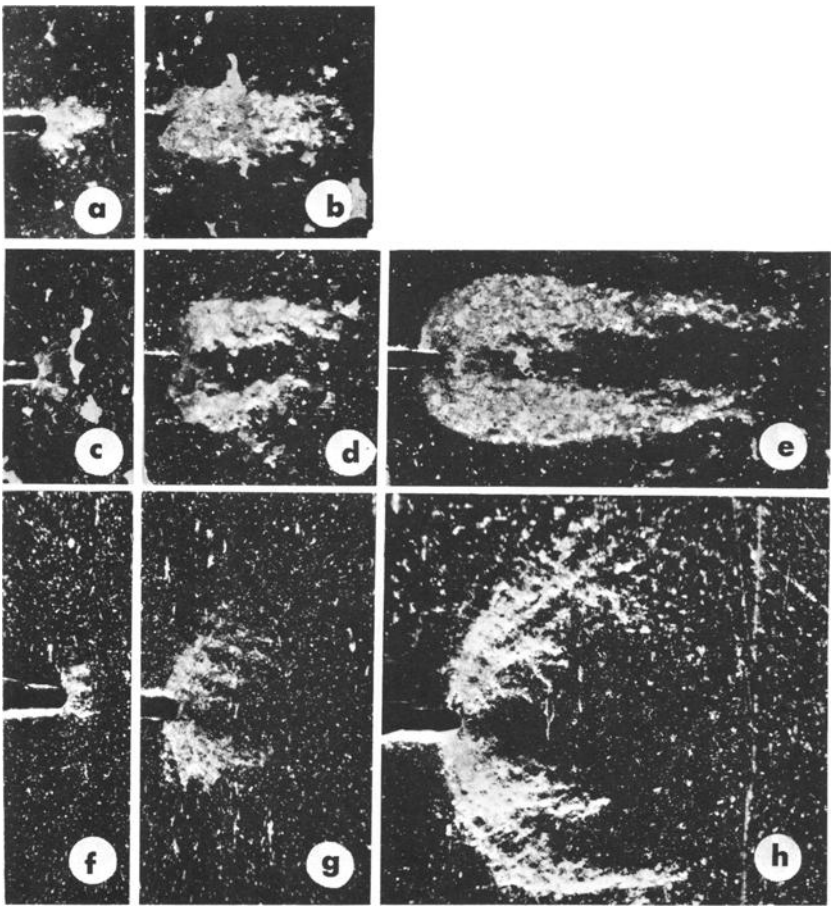

(*a*) [6.4] t = 0.017 in. (0.43 mm)
(*b*) [14] t = 0.017 in. (0.43 mm)
(*c*) [1.1] t = 0.058 in. (1.5 mm)
(*d*) [4.2] t = 0.058 in. (1.5 mm)
(*e*) [8.2] t = 0.058 in. (1.5 mm)
(*f*) [0.54] t = 0.200 in. (5.1 mm)
(*g*) [1.2] t = 0.200 in. (5.1 mm)
(*h*) [2.1] t = 0.200 in. (5.1 mm)
(*i*) [2.7] t = 0.200 in. (5.1 mm)

FIG. 12—*Influence of stress level and thickness on the appearance of plastic zones revealed by etching edge-notched Fe-3Si steel plates. Photographs show zones etched on plate surface. Oblique lighting* (×*9.5*). *The numbers in the brackets are the values of* $(K/Y)^2 1/t$.

graphically for three different crack lengths in Fig. 11. As shown in Fig. 11*b*, it is in good accord with upper limits for plane strain deduced from K_{Ic} measurements. The limiting condition proposed by Brown and Srawley (see Fig. 11*b* and Table 3) is similar but more conservative [*16*].

The plastic zone is a mixture of plane strain and plane stress relaxation when $\rho_{(\text{plane strain})} = t/2$ or $(K/Y)^2\ 1/t = 2.6$, and this can be seen in Fig. 12*h* and *i*. The zones revealed by etching show that the deformation occurring when $\rho_{(\text{plane stress})} = 2t$ is mainly of the through-the-thickness variety (see Fig. 10*d*), and this is a tentative and approximate lower limit for plane stress. However, at this stage much of the accumulated deformation is still of the plane strain variety. Consequently, ρ at fracture must be even larger, that is, $>4t$, for the fracture to have a

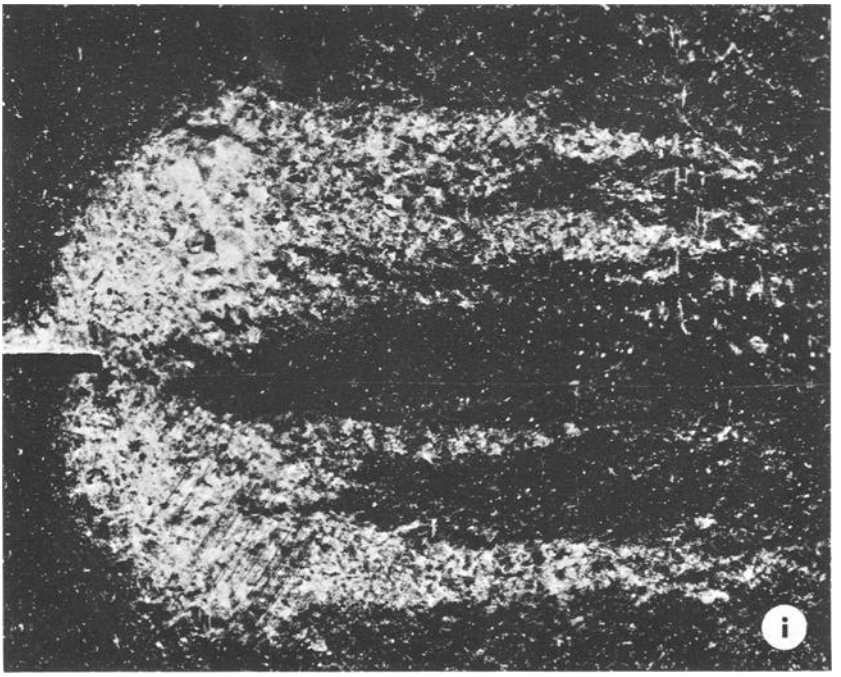

FIG. 12—(*Continued.*)

strong history of plane stress, consistent with the definition of K_c used here.[4] These limits are summarized in Table 3 and graphed in Fig. 11.

Strain and Strain Hardening

The expressions for crack-tip displacement, Eqs 8 and 9, are the simplified elastic-plastic counterparts of Eq 1. However, the displacement values only become meaningful to the metallurgist when they are converted to local plastic strain. This can be done approximately with the help of additional experimental inputs. For example, the etching results (Figs. 3 and 4) suggest that the plane strain zone can be modeled by two regions of shear. Near the crack tip these regions overlap and have a finite width l, as shown in Fig. 9. In a similar way, plane stress zones

can also be characterized by a finite width l (see Fig. 9). The value of l is *not* a constant for each type of zone but depends on stress level and strain hardening rate. For example, plane strain zones reproduced in Fig. 4 show $l \backsim 0.002$ in. (0.5 mm) for $K/Y = 0.3\ t$ and $l \backsim 0.005$ in. (1.3 mm) for $K/Y = 0.45$. The influence of strain hardening may be even more important. Figure 6 illustrates systematic changes in the shape of the plane stress zone that accompany changes in n, the strain hardening exponent. Such an increase in l and the accompanying decrease in the strain concentration at the crack tip was first noted by Gerberich [*12*], and other examples can be found in his paper. Although evidence of this kind for plane strain zones is lacking, a similar effect is to be expected, and this is shown schematically in Fig. 9*c*.

Etched zones also show that the strain is not uniform across the sheared region. In the calculations that follow a linear shear strain gradient is assumed, but this is merely a crude, first approximation. The situation is made even more complicated under plane stress by the necking instability that usually precedes crack extension. This tends to confine strain in the final stages of loading to a region comparable to the sheet thickness. To emphasize the fact that l is related to strain hardening and thickness the symbols $l_{(n)}$ and $l_{(n,t)}$ are used to denote the zone width under plane strain and plane stress, respectively.

As shown in Fig. 9*b*, $\bar{\gamma}_c$, the average shear strain at the crack tip in one of the sheared regions is [*9*]:

$$\bar{\gamma}_c \approx \frac{v_c}{l_{(n)}}; \quad \ldots\ldots\ldots\ldots\ldots\ldots\ldots\ldots (10)$$

The average tensile strain $\bar{\epsilon}_c$ in the region where the zones overlap is:

$$\bar{\epsilon}_c \approx \frac{v_c}{l_{(n)}} \quad \ldots\ldots\ldots\ldots\ldots\ldots\ldots\ldots (11)$$

Assuming that the distribution of strain is linear, ϵ_c the peak crack tip strain is:

$$\epsilon_c \approx 2\bar{\epsilon}_c, \quad \ldots\ldots\ldots\ldots\ldots\ldots\ldots\ldots (12)$$

combining Eqs 8, 11, and 12 gives the sought-for result:

$$\text{plane strain } \epsilon_c \approx \frac{Y}{2l_{(n)}E}\left(\frac{K}{Y}\right)^2. \quad \ldots\ldots\ldots\ldots\ldots (13)$$

For plane stress, we have shown [*11*] that $\bar{\epsilon}_c \approx 2v_c/l_{(n)}$ and by a similar argument to that used in deriving Eq 13:

$$\text{plane stress } \epsilon_c \approx \frac{2Y}{l_{(n,t)}E}\left(\frac{K}{Y}\right)^2 \quad \ldots\ldots\ldots\ldots\ldots (14)$$

Evidence that Eq 13 can offer reasonable estimates of the local strain

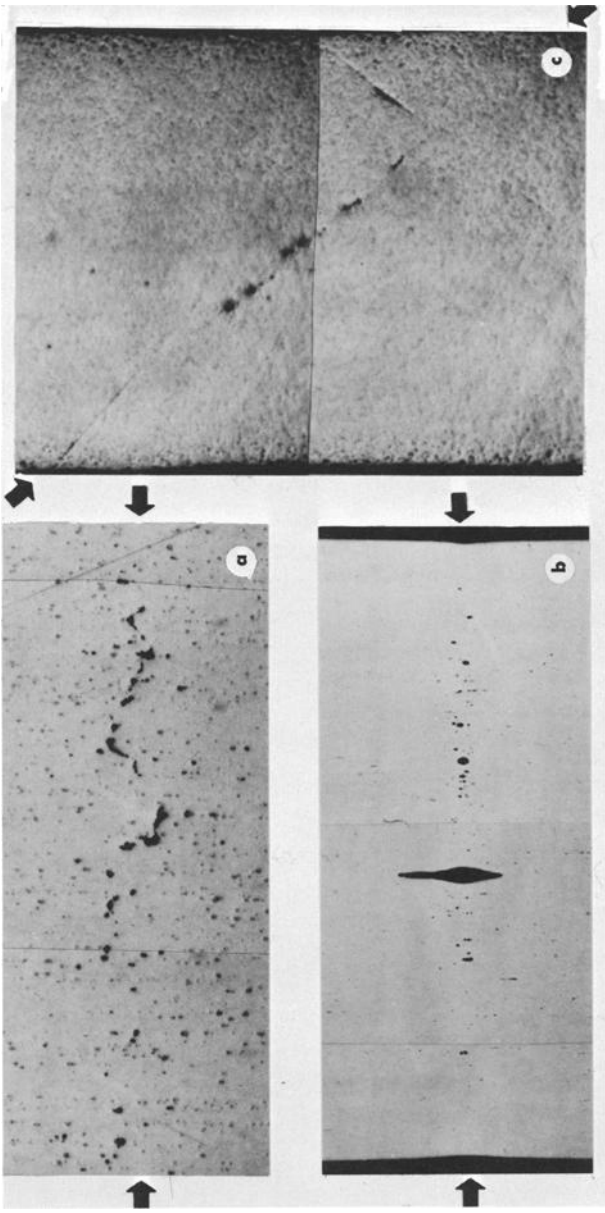

(a) 7075-T6 aluminum, Y = 73 ksi (51 kg/mm²), reduction of area = 35 per cent, K = 42 *ksi* $\sqrt{\text{in.}}$ (150 kgf/mm$^{3/2}$), $(K/Y)^2 1/t$ = 3.5. Section taken 0.006 in. (1.5 mm) from the crack tip (×100). (b) Mild steel, Y = 41 ksi (29 kgf/mm²), reduction of area = 56 per cent, K = 37 ksi $\sqrt{\text{in.}}$ (132 kgf/mm$^{3/2}$), $(K/Y)^2 1/t$ = 1.6. Section taken 0.002 in. (0.5 mm) from the crack tip (×10). (c) Ti-6Al-4 *V*, Y = 139 ksi (98 kgf/mm²), reduction of area = 46 per cent, K = 155 ksi $\sqrt{\text{in.}}$ (550 kgf/mm$^{3/2}$), $(K/Y)^2 1/t$ = 30. Section taken near the tip of a slowly growing crack 0.041 in. (1 mm) from the notch (×100).

FIG. 13—*Metallographic evidence of incipient cracking displayed by stressed but unbroken plates in the heavily deformed region ahead of a sharp notch. Sections are normal to the plate surface and the crack plane (the latter is indicated by arrows).*

at low stress levels, that is, $T/Y < 0.7$ is contained in Appendix B, Ref 9. Equation 14 is less accurate, and both expressions should be regarded only as first approximations.

Ductile Fracture Criteria

Ductile fracture frequently involves the nucleation of voids and the linking up of these voids to form a crack. Several examples of incipient ductile cracking in the heavily strained region just ahead of a crack are reproduced in Fig. 13. McClintock [*18,19*] has recently calculated the critical true strain, $\bar{\epsilon}^*$ that will expand a system of cylindrical void

TABLE 4—*Stress states and corresponding ductility values.*

Type	$(\sigma_{max} + \sigma_T)/\bar{\sigma}$	$\bar{\epsilon}^*/\epsilon^*$(tension test)	
		Calculated,[e]	Measured,[f]
Round tensile bar (with necking)	1 to 1.7[a]	1.0	...
Pure plane stress[b]	1.5	1.0	...
Plane stress zone[c] (with necking in the thickness direction)	~2.1	~0.65	0.52,[g] 0.52,[h] 0.39[i]
Plane strain zone[d] (maximum constraint)	~4.7	~0.10	...

$\bar{\epsilon}^*$ True fracture strain.

[a] Calculated from Ref *10* for $\bar{\epsilon}^* = 0$ to 1.0.

[b] $\sigma_1 = \bar{\sigma}$, $\sigma_2 = \frac{1}{2}\bar{\sigma}$, $\sigma_3 = 0$, ϵ_1 , $\epsilon_2 = 0$, $\epsilon_3 = -\epsilon_1$.

[c] $\sigma_1 = 1.3\bar{\sigma}$, $\sigma_2 = 0.8\bar{\sigma}$, $\sigma_3 = 0.3\bar{\sigma}$, ϵ_1 , $\epsilon_2 = 0$, $\epsilon_3 = -\epsilon_1$.

[d] $\sigma_1 = 2.6\bar{\sigma}$, $\sigma_2 = 2.1\bar{\sigma}$, $\sigma_3 = 1.6\bar{\sigma}$, ϵ_1 , $\epsilon_2 = 0$, $\epsilon_3 = -\epsilon_1$.

[e] Calculated for Refs *18, 19*.

[f] Measured at the midsection of a deep, blunt-notched sheet coupon, notch root radius = $2t$.

[g] 2219-T86 Al: $Y = 59$ ksi, $\bar{\epsilon}^*_{(\text{tension test})} = 0.45$, $n = 0.085$.

[h] 7075-T6 Al: $Y = 73$ ksi, $\bar{\epsilon}^*_{(\text{tension test})} = 0.45$, $n = 0.061$.

[i] Type 4340 steel: $Y = 189$ ksi, $\bar{\epsilon}^*_{(\text{tension test})} = 0.60$, $n = 0.064$.

nuclei to the stage where the voids link-up. These calculations indicate that ϵ^* is markedly reduced by a triaxial stress state, that is, large values of $(\sigma_{max} + \sigma_T)/\bar{\sigma}$ where σ_{max} is the normal stress, σ_T the transverse stress (normal to the cylinder axis) and $\bar{\sigma}$ the flow stress. Table 4 compares the stress state in uniaxial tension with that existing in the plane stress and plane strain plastic zone ahead of a crack, and the corresponding critical strain values derived from the McClintock treatment. Experimental results for deep blunt-notched sheet coupons (which approximate the plane stress zone) are also quoted, and these tend to support the calculations. However, the large reduction in the ductility of material within a plane strain zone is difficult to check and open to question. For one thing, there is some evidence that full triaxiality is not attained immediately [*9*]. Even if it is, the triaxiality will be generated near the elastic-plastic boundary where the plastic strain is small (near A in Fig. 9*b*), while the peak strains will occur near the root of the crack

(near B in Fig. 9*b*) where a plane stress state prevails. Consequently, the ductility under plane strain may be quite similar to plane stress. There are further complications because of the directionality of properties. It is well known that flat rolled products are weakest in the thickness direction. Whereas a transverse stress is developed in this direction under plane strain, no such stress is developed under plane stress. On this basis the following are not unreasonable as first approximations:

$$\bar{\epsilon}^*_{(\text{ahead of a crack})} \propto \bar{\epsilon}^*_{(\text{tension test})} \quad \ldots\ldots\ldots\ldots (15a)$$

and

$$\bar{\epsilon}^*_{(\text{plane strain zone})} \backsim (1/3)\bar{\epsilon}^*_{(\text{tension test})} \quad \ldots\ldots\ldots\ldots (15b)$$

TABLE 5—*Summary of K_{Ic}, tensile properties and the $l_{(n)}$ values calculated for a number of aluminum, titanium, and steel alloys.*

Alloy, References	E, ksi	Y, ksi	K_{Ic},[b] ksi-in.$^{1/2}$	ϵ^*	n	$l^*_{(n)}$ (in.) Calculated
2219-T87 [*20,22*]	1.0×10^4	59	33	0.39	0.085	7.1×10^{-3}
7075-T6 [*20,21,24,26*]	1.0	73	37	0.34	0.061	6.5×10^{-3}
2014-T6 [*24*]	1.0	68	35	0.37	0.08	7.5×10^{-3}
2024-T4 [*15,26*]	1.0	50	59	0.32	0.16	3.2×10^{-2}
Ti-8Al-1Mo-1V [*25*]	1.7	145	76	0.34	0.11	1.00×10^{-2}
Ti-6Al-4V [*24,25*]	1.7	138	49	0.56	0.05	2.7×10^{-3}
Ti-5Al-2.5Sn ELI[a] [*27*]	1.7	170	60	0.36	0.06	4.6×10^{-3}
4330M [*20,23*]	3.0	189	90	0.60	0.064	3.5×10^{-3}
18Ni Maraging [*28,29*]	3.0	275	70	0.76	0.013	7.8×10^{-4}
4340(400) [*28,30*]	3.0	210	65	0.60	0.056	1.7×10^{-3}
4340(600) [*28,30*]	3.0	200	65	0.80	0.028	1.3×10^{-3}

[a] −196 C.

[b] K_{Ic} may be expressed in metric form by multiplying the values in this Table by 3.57 to obtain the value in kgf/mm$^{3/2}$.

and

$$\bar{\epsilon}^*_{(\text{plane stress zone})} \backsim (1/2)\bar{\epsilon}^*_{(\text{tension test})} \quad \ldots\ldots\ldots\ldots (15c)$$

Although only Eq 15*a* is essential to the argument presented here, it is probably the crudest of the assumptions made and the largest source of error.

Calculating Fracture Toughness

The parameters K_{Ic} and K_c can now be formulated by combining Eqs 13 and 14, the expressions for the peak strain, with Eqs 15*b* and 15*c* which describes the critical strain for ductile rupture, and by noting that, by definition, K_{Ic}, $K_c = K_{(\epsilon_c = \epsilon^*)}$:

$$K_{Ic} \approx \sqrt{(2/3)EYl^*_{(n)}\bar{\epsilon}^*} \quad \ldots\ldots\ldots\ldots (16)$$

$$K_c \approx \sqrt{(1/4)EYl^*_{(n,t)}\bar{\epsilon}^*} \quad \ldots\ldots\ldots\ldots (17)$$

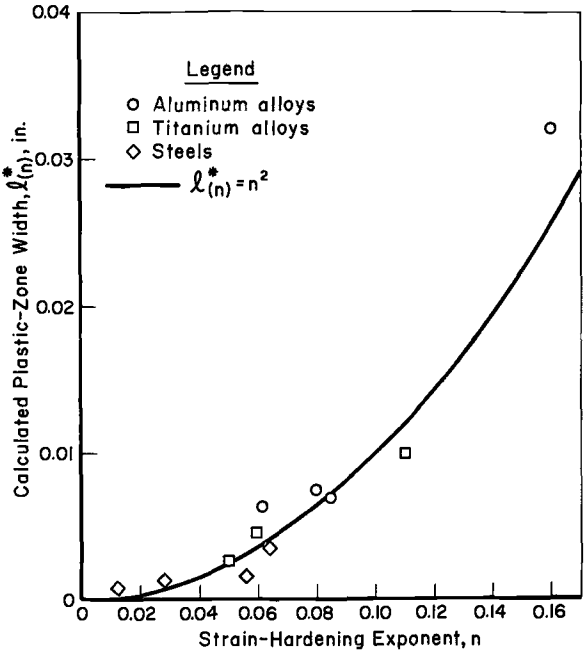

FIG. 14—*Relation between calculated values of the plastic zone width* $l^*_{(n)}$, *and the strain hardening index for the alloys in Table 5.*

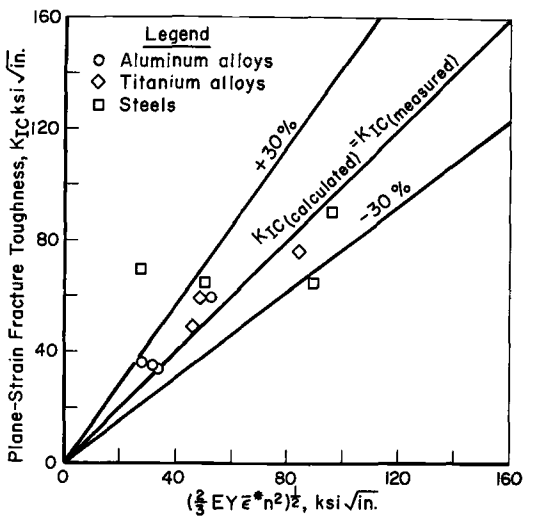

FIG. 15—*Comparison of measured* K_{Ic} *values with values calculated from ordinary tensile properties with Eq 19.*

where $l^*_{(n)}$ and $l^*_{(n,t)}$ are the values of l at the onset of cracking. One way of testing these expressions is to calculate the value of l^* when K_{Ic} (or K_c) E, Y and $\bar{\epsilon}^*$ are known and compare this value with measurements. This is done in Table 5 for a number of alloys for which K_{Ic},

E, Y, $\bar{\epsilon}^*$ and n are known. Most of the values range from $l^*_{(n)} = 0.001$ to 0.007 in. (0.25 to 1.8 mm), and this agrees with the value of l displayed by plane strain zones in Fe-3Si steel at comparable K/Y levels. This supports the idea that the value of $l^*_{(n)}$ is not artificial but has a physical basis.

The value of $l^*_{(n)}$ should also depend on strain hardening, and this is also borne out. When the $l^*_{(n)}$ values calculated for eleven different alloys are plotted in Fig. 14 against n, the strain hardening exponent, a correlation is obtained:

$$l^*_{(n)} \text{ (inches)} \approx n^2 \quad \ldots\ldots\ldots\ldots\ldots\ldots (18)$$

This correlation not only contains the effect of n on $l^*_{(n)}$ but makes adjustments for: (*a*) the effects of n on the flow stress, on ν_c and on the ductility criterion, and (*b*) any errors in the assumptions for $\bar{\gamma}$ and ϵ_c.

The term $l^*_{(n)}$ can now be replaced by n^2 in Eq 16:

$$K_{Ic} \approx \sqrt{(\tfrac{2}{3})EY\bar{\epsilon}^* n^2} \quad \ldots\ldots\ldots\ldots\ldots\ldots (19)$$

Figure 15 shows that all but one of the measured K_{Ic} values in Table 5 can be predicted from tensile properties to within $\pm$ about 30 per cent with this expression. The one exception is the 18 per cent nickel maraging steel which has an unusually low strain hardening exponent (n = 0.013). The value quoted may be in error. Alternatively, a more complicated form of Eq 18, that is, $l^*_{(n)} \approx (0.0005 + n^2)$ inches, is more appropriate when $n < 0.02$, and if this were used all the values would fall within the $\pm$30 per cent limits. In view of the relatively small volume of data drawn on by the correlation, this refinement is probably not yet warranted. The precision with which the calculations match the experiments must be regarded as very good considering: (*a*) that measured K_{Ic} values frequently vary from specimen to specimen and laboratory to laboratory by more than $\pm$10 per cent, (*b*) that the n values used may not be exact, and (*c*) that strain hardening effects have been neglected until the very end. Finally, it should be noted that the same approach can be used to formulate the value of $l^*_{(n,t)}$, when more K_c values (as defined here) become available.

Discussion

The conclusion that strain hardening has an important influence on crack extension resistance is not new; Krafft [*31*] and Krafft and Irwin [*32*] have also proposed that $K_{Ic} \propto n$, but arrive at this conclusion by a different route.[7] Other data supporting a linear relation between K_{Ic} and n have been reported by Lauta and Steigerwald [*28*].

[7] Krafft [*31*] assumes that $\epsilon^* = n$ and that the elastic strain gradient is valid near the crack tip. This gives the result: $K_{Ic} = \sqrt{2\pi E^2 n^2 d_t}$ where $r_{(\epsilon=n)} \equiv d_t$, and d_t is regarded as a ligament spacing. The difficulty with this approach is that the assumptions are open to question.

The role of strain hardening helps to explain the general effect of heat treating on K_{Ic}. Higher yield stress values are usually obtained in this way at the expense of strain hardening (and sometimes at the cost of ductility). The differential form of Eq 19:

$$\frac{\Delta K_{Ic}}{K_{Ic}} = \frac{1}{2}\frac{\Delta Y}{Y} + \frac{1}{2}\frac{\Delta \bar{\epsilon}^*}{\bar{\epsilon}^*} + \frac{\Delta n}{n} \quad \ldots\ldots\ldots\ldots (20)$$

shows that the value of K_{Ic} tends to fall unless the fractional increase in yield stress is twice the accompanying decrease in n. The data reproduced in Fig. 16*a* and *b* illustrate this effect. Figure 16*a* reproduces the tensile properties of 4340 steel tempered at different temperatures from 375 to

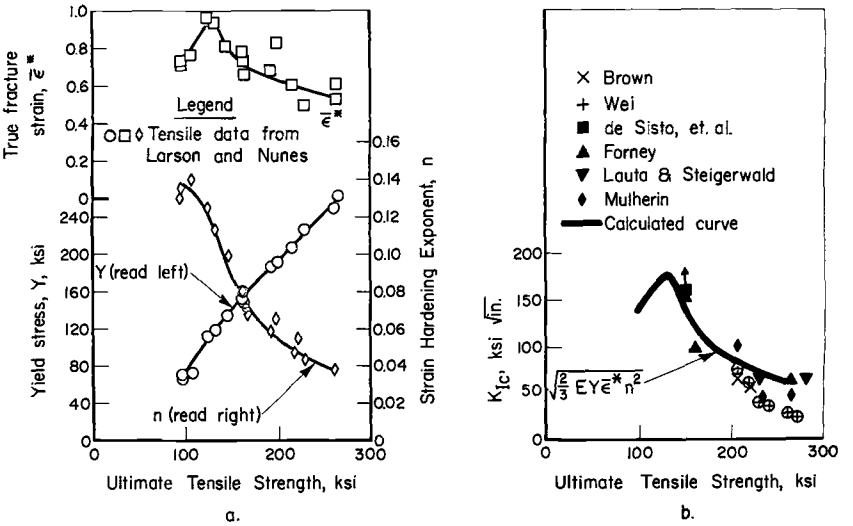

FIG. 16—*Properties of Type 4340 steel heat treated to different strength levels:* (a) *tensile properties reported by Larson and Nunes* [30] *and* (b) K_{Ic} *values calculated from* (a) *and measured by different investigators* [16,24,28,30,33–35].

1200 F (190 to 650 C). Over this range the yield stress shows a 4-fold increase, n a 3½-fold decrease, and $\bar{\epsilon}^*$ shows increases and decreases. These properties were used to calculate K_{Ic}, and the results are compared with actual measurements taken from the literature. The agreement is reasonably good considering that the comparison involves different heats of Type 4340. They show the expected trend to lower K_{Ic} values at the higher strength levels, and this is associated mainly with the reduced strain hardening. Discrepancies at the highest stress levels may be caused by the onset of a "cleavage-type" fracture mechanism [*36*] that does not obey a strain criterion. Figure 16 illustrates another advantage of Eg 19. By relating K_{Ic} with the ordinary tensile properties, it offers a way of bringing existing metallurgical experience to bear on fracture toughness problems. The K_{Ic} values of new alloys can be anticipated. The prospect

of a higher strength level can be weighed against a projected reduction in K_{Ic}. Effects of composition, microstructure, and even texture may be interpreted more easily. In some cases, it may be possible to insure a minimum K_{Ic} level by specifying permissible variations in the tensile properties. Finally, the analysis draws attention to the important role of ductility and especially strain hardening rate (or the yield to ultimate ratio which is closely related to n) and the need for improving these along with yield stress to produce even tougher alloys.

Conclusions

1. This paper identifies four basic factors that contribute to the fracture toughness of metals: (*a*) the character of plastic relaxation at the crack tip—whether it is plane strain or plane stress, (*b*) the amount of plastic flow near the crack tip, (*c*) the peak strain generated, and (*d*) the critical strain for ductile rupture. These factors can be described numerically with the aid of two simplified elastic-plastic treatments.

2. The character of relaxation depends on the size of the plastic zone relative to the plate thickness. The absolute size of the zone $\rho \propto (K/Y)^2$.

3. The amount of flow is described in terms of a crack-tip displacement $v_c \propto Y/E(K/Y)^2$.

4. The peak strain is determined by the way the deformation is distributed. This is characterized by the dimension $l_{(n)}$, the width of the plastic zone close to the crack tip under plane strain, which depends on the strain hardening exponent, $l_{(n)} \propto n^2$. The peak strain $\epsilon_c \propto V_c/l_{(n)}$.

5. The critical true strain for coalescing voids $\bar{\epsilon}^*$ depends on the microstructure and state of stress and is related to the true strain at fracture displayed by ordinary tension specimens: $\bar{\epsilon}^*$ (ahead of a crack) $\propto \bar{\epsilon}^*$ (tension test).

6. The plane strain fracture toughness parameter K_{Ic} can be expressed in terms of ordinary tensile properties by combining the various descriptions and correlating the result with existing measurements: $K_{Ic} \approx \sqrt{\frac{2}{3}EY\bar{\epsilon}^* n^2}$. The expression is accurate to within about ± 30 per cent for eleven different aluminum, titanium, and steel alloys and offers useful insights to the metallurgical origins of K_{Ic}.

Acknowledgments

The authors wish to thank the Strength and Dynamics Branch of the Air Force Materials Laboratory, especially W. J. Trapp and A. W. Brisbane, for supporting the preparation of this report. They have drawn on research sponsored at Battelle Memorial Institute by this agency, The Ship Structure Committee, and The Army Research Office, and work for the American Gas Association which has previously been reported. The authors are grateful for the support of these groups. They also wish to thank R. I. Jaffee for his encouragement; A. K. Mukherjee,

P. N. Mincer, R. L. Stephenson, R. C. Barnes, T. L. Buckner, J. S. Duerr, and J. L. McCall, who made important contributions to the unpublished experimental work that is reported; and Carolyn Pepper for her help in preparing the manuscript.

References

[1] *Fracture Toughness Testing and Its Applications, ASTM STP 381,* American Society for Testing and Materials, 1965.

[2] Hahn, G. T. and Rosenfield, A. R., "Mechanics and Metallurgy of Brittle Crack Extension," *Proceedings of the American Society of Civil Engineers, Engineering Mechanics Division Specialty Conference,* Washington, D. C., Oct. 1966.

[3] Inglis, C. E., "Stresses in a Plate Due to the Presence of Cracks and Sharp Corners," *Transactions of the Institute of Naval Architects,* Vol. 55, 1913, p. 219.

[4] Bilby, B. A. and Swinden, K. H., "Representation of Plasticity at Notches by Linear Dislocation Arrays," *Proceeding,* Royal Society of London, Vol. 285, 1965, p. 22.

[5] Rice, J. R., "The Mechanics of Crack Tip Deformation and Extension by Fatigue," Brown University Report on NSF Research Grant GK 286, May 1966.

[6] Dugdale, D. S., "Yielding of Steel Sheets Containing Slits," *Journal of the Mechanics and Physics of Solids,* Vol. 8, 1960, p. 100.

[7] McClintock, F. A. and Irwin, G. R., "Plasticity Aspects of the Fracture Mechanics," *Fracture Toughness Testing and Its Applications, ASTM STP 381,* American Society for Testing and Materials, 1965, p. 84.

[8] Davis, P. C. and Sih, G. C., "Stress Analysis of Cracks," *Fracture Toughness Testing and Its Applications, ASTM STP 381,* American Society for Testing and Materials, 1965, p. 30.

[9] Hahn, G. T. and Rosenfield, A. R., "Experimental Determination of Plastic Constraint Ahead of a Sharp Crack Under Plane-Strain Conditions," *Transactions,* American Society for Metals, Vol. 59, 1966, p. 909.

[10] Bridgman, P. W., *Studies in Large Plastic Flow and Fracture,* Harvard Press, Cambridge, Mass., 1964.

[11] Rosenfield, A. R., Dai, P. K., and Hahn, G. T., "Crack Extension and Propagation Under Plane Stress," *Proceedings of the First International Conference on Fracture,* Vol. 1, 1965, p. 223.

[12] Gerberich, W. W. "Plastic Strains and Energy Density in Cracked Plates, Part I, Experimental Techniques and Results," *Experimental Mechanics,* Vol. 4, 1964, p. 335.

[13] Wells, A. A., "Notched Bar Tests, Fracture Mechanics and Strength of Welded Structures," *British Welding Journal,* Vol. 12, No. 1, Jan. 1965.

[14] Tetelman, A. S., "The Effect of Plastic Strain and Temperature on Microcrack Propagation in Iron—3% Silicon," *Acta Metallurgica,* Vol. 12, 1964, p. 993.

[15] Irwin, G. R., "Fracture Mode Transition for a Crack Traversing a Plate," *Transactions,* American Society of Mechanical Engineers, Series D, Vol. 82, 1960, p. 417.

[16] Brown, W. F. Jr., and Srawley, J. E., "Current Status of Plane Crack Toughness Testing," Technical Memorandum NASA TMX-52209, June 29, 1966.

[17] Jones, M. H., Fisher, D. M., and Brown, W. F., Jr., "Progress Report on NASA-NRL Cooperative Fracture Testing Program," Oct. 12, 1966, also Jan. 23, 1967.

[18] McClintock, F. A., "A Criterion for Ductile Rupture," (to be published).

[19] Rosenfield, A. R. and Hahn, G. T., "Numerical Descriptions of the Ambient Low-Temperature, and High-Strain Rate Flow and Fracture Behavior of

Plain Carbon Steel," *Transactions*, American Society for Metals, Vol. 59, 1966, p. 962.

[*20*] Mukherjee, A. K. et al, "Notch Behavior in Metals," AFML-TR-66-266, Air Force Materials Laboratory Report, 1966.

[*21*] Boyle, R. W., Sullivan, A. M., and Krafft, J. M., "Determination of Plain Strain Fracture Toughness with Sharply Notched Sheets," *Welding Journal*, Vol. 41, 1962, pp. 428s–432s.

[*22*] Tiffany, C. F., Lorenz, P. M., and Hall, L. R., "Investigation of Plane-Strain Flow Growth in Thick Walled Tanks," *NASA* CR-54837, NASA Report, Feb. 1966.

[*23*] Irwin, G. R. and Srawley, J. E., "Progress in The Development of Crack Toughness Fracture Tests," Presented to the Deutsches Verband für Material prufüng, Würzburg Meeting, March 1961.

[*24*] Forney, J. W., "Fracture Toughness Evaluation of Titanium," Aluminum and Steel, Memorandum Report M66-20-1 (AD632926), Frankford Arsenal, 1966.

[*25*] De Sisto, T. S., "The True Stress True Strain Properties of Titanium and Titanium Alloys as a Function of Temperature and Strain Rate," Report No. WAL-TR-405.2/4, Watertown Arsenal, 1959.

[*26*] Kaufman, J. G., "True Stress-Strain Properties of Aluminum Alloys," Report No. 9-61-32, Alcoa Research Laboratory, Oct. 1961.

[*27*] Carman, C. M., Forney, J. W., and Katlin, J. M., "Plane Strain Fracture Toughness and Mechanical Properties of 5A1-2.5Sn ELI Titanium at Room and Cryogenic Temperatures," FA Report R-1796, Frankford Arsenal, April 1966.

[*28*] Lauta, F. J. and Steigerwald, E. A., "Influence of Work Hardening Coefficient on Crack Propagation in High-Strength Steels," AFML-TR-65-31, Air Force Materials Laboratory, May 1965.

[*29*] Kula, E. B. and Hicky, C. F., "Evolution of Maraging Steels at The Army Materials Research Agency," Third Maraging Steel Project Review, RTD-TDR-63-4048, Air Force Materials Laboratory, Nov. 1963, p. 439.

[*30*] Larson, F. R. and Nunes, J., "Low Temperatures Flow and Fracture Tension Properties of Heat Treated SAE 4340 Steel," *Transactions*, Amercian Society for Metals, Vol. 53, 1961, p. 663.

[*31*] Krafft, J. M., "Correlation of Plane Strain Crack Toughness with Strain Hardening Characteristics of a Low, a Medium, and a High-Strength Steel," *Applied Materials Research*, Vol. 3, 1963, p. 88.

[*32*] Krafft, J. M. and Irwin, G. R., "Crack Velocity Considerations," *Fracture Toughness Testing and Its Applications, ASTM STP 381*, American Society for Testing and Materials, 1965, p. 84.

[*33*] Wei, R. P., "Fracture Toughness Testing in Alloy Development," *Fracture Toughness Testing and Its Applications, ASTM STP 381*, American Society for Testing and Materials, 1965, p. 279.

[*34*] De Sisto, T. S., Carr, F. L., and Larson, F. R., "The Influence of Section Size on the Mechanical Properties and Fracture Toughness of 7075-T6 Aluminum, 6Al-6V-2Si Titanium and AlS1 4340 Steel," AMRATR64-05 Army Mats. Res. Agency, 1964.

[*35*] Mulherin, J. H., "Stress-Corrosion Susceptibility of High-Strength Steel, in Relation to Fracture Toughness," *Transactions*, American Society of Mechanical Engineers, 1967 (Paper 66-Met-5).

[*36*] Shih, C. H., Averbach, B. L., and Cohen, M., "Some Effects of Silicon on the Mechanical Properties of High-Strength Steels," *Transactions*, American Society for Metals, Vol. 48, 1956, p. 86.